*Vlado A. Lubarda** and *Marc A. Meyers***

ON PLASTIC VOID GROWTH IN STRONG DUCTILE MATERIALS

Abstract

An elastoplastic analysis of spherical and cylidrical void growth under uniform tension is presented. The stress dependence on the void size is derived for an ideally plastic and an incompressible elastic–linearly hardening material, accurate to first order in the ratio of the plastic hardening rate and the elastic modulus. The critical stress is calculated at which an unstable cavitation takes place for selected material properties. The implications to spalling strength of strong ductile materials are discussed, with a particular referral to nanocrystalline materials processed by severe plastic deformation and characterized by exceedingly high values of the hardening rate. Relationship to earlier work on the subject is also given.

*Prof. dr V.A. Lubarda, The Montenegrin Academy of Sciences and Arts, 81000 Podgorica, SCG, and University of California, San Diego, CA 92093-0411, USA.

**Prof. dr M.A. Meyers, Department of Mechanical and Aerospace Engineering, University of California, San Diego, CA 92093-0411, USA.

O PLASTIČNOM PORASTU PRAZNINA U ČVRSTIM MATERIJALIMA

I z v o d

U radu je data elastoplastična analiza porasta sfernih i cilindričnih praznina u čvrstim žilavim materijalima. Izveden je izraz za napon u zavisnosti od poluprečnika praznine u nekompresibilnom elastoplastičnom materijalu sa linearnim očvršćavanjem, sa tačnošću prvog reda u odnosu na količnik modula očvršćavanja i elastičnosti. Granična vrijednost napona pri kojoj se javlja kavitaciona nestabilnost je sračunata za izabrana materijalna svojstva. Značaj rezultata za procjenu izdržljivosti materijala pri dinamičkim opterećenjima je diskutovan, uz poseban akcenat na nanokristalne materijale procesovane intenzivnom plastičnom deformacijom i okarakterisane izuzetno visokim modulom očvršćavanja. Osvrt na ranija istraživanja je takodje dat.

1. INTRODUCTION

A study of the nucleation and growth of voids in ductile metals is of significant interest for understanding of the material failure under overall tensile loading. Such failure can occur upon reflection of tensile waves from the free surface of impacted plate which leads to its spalling (Fig. 1), or near the crack tip, and in the center of a necked specimen (Meyers and Aimone, 1983; Meyers, Murr and Staudhammer, 1986; Tvergaard, 1990). Both analytical and computational research were devoted to analyze the void growth and coalescence in different materials and under different loading conditions. The representative references include McClintock (1968), Rice and Tracey (1969), Needleman (1972), Gurson (1977), Budiansky, Hutchinson and Slutsky (1982), Koplik and Needleman (1988), Huang, Hutchinson and Tvergaard (1991), Needleman, Tvergaard and Hutchinson (1992), Cuitiño and Ortiz (1996), Pardoen and Hutchinson (2000), Lubarda, Schneider, Meyers *et al.* (2003), and Kassner and Hayes (2003). Dynamic expansion of cavities in elastoplastic metals was studied by Hopkins (1960), Carroll and
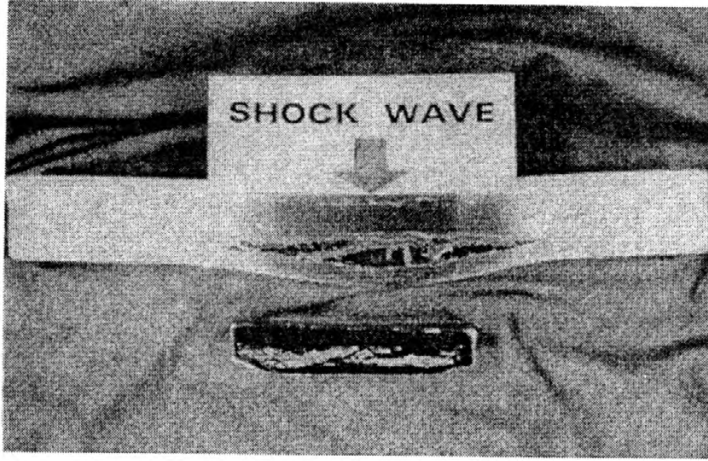
Figure 1: Spalling of plate under shock loading, produced by growth and coalescence of voids near rear end of the plate. Two completely spalled plates are shown, after being sectioned: the upper photo is for AISI 1008 steel plate, and the lower is for nickel plate (from Meyers and Aimone, 1983).

Holt (1972), Johnson (1981), Cortés (1992), Ortiz and Molinari (1992), Benson (1993), Wang (1994), Wu, Ramesh and Wright (2003), and others. The void growth in nonlinear hyperelastic materials was considered by Williams and Schapery (1965), Ball (1982), Stuart (1985), Horgan (1992), Polignone and Horgan (1993), and Horgan and Polignone (1996). There has also been a recent effort devoted to the analysis of void growth by using the atomistic simulations (e.g., Belak, 1998; Rudd and Belak, 2002).

In this paper we present an elastoplastic analysis of spherical void growth under remote triaxial tension, which is analogous to classical analysis of the void growth under internal void pressure (Hill, 1950; Chakrabarty, 1987; Lubliner, 1990). Analytical formulas are derived for the applied stress in terms of the void size at any stage of finite plastic deformation. The accuracy of the order k/E is retained in the derivation, where k is the hardening modulus and E is the elastic

modulus of the material. The bifurcation stress for the nucleation of the void, or the limiting stress for cavitation instability of the pre-existing void, are calculated for selected material properties. The corresponding results for the growth of cylindrical void are also presented. The implications on the spalling strength of strong materials under dynamic loading are discussed, with a particular referral to nanocrystalline materials processed by severe plastic deformation and characterized by exceedingly high values of the hardening rate.

2. SPHERICAL VOID GROWTH

Consider a spherical void of initial radius R_0 in an isotropic infinite medium under remote triaxial tension σ. The stress state at an arbitrary point consists of the radial stress σ_r and the hoop stress $\sigma_\theta = \sigma_\phi$. Due to spherical symmetry, the stress components depend only on the radial distance r, and not on the spherical angles θ and ϕ. In the absence of body forces the equilibrium equation is

$$\frac{d\sigma_r}{dr} - \frac{2}{r}(\sigma_\theta - \sigma_r) = 0 .\qquad(2.1)$$

If the material response is within the infinitesimal elastic range, the compatibility equation reduces to

$$\frac{d}{dr}(\sigma_r + 2\sigma_\theta) = 0 ,\qquad(2.2)$$

which implies that the spherical component of stress tensor is uniform throughout the medium, and thus equal to σ, i.e.,

$$\sigma_r + 2\sigma_\theta = 3\sigma .\qquad(2.3)$$

Combining Eqs. (2.1) and (2.3) it follows that

$$\sigma_r = \sigma\left(1 - \frac{R_0^3}{r^3}\right), \quad \sigma_\theta = \sigma\left(1 + \frac{1}{2}\frac{R_0^3}{r^3}\right).\qquad(2.4)$$
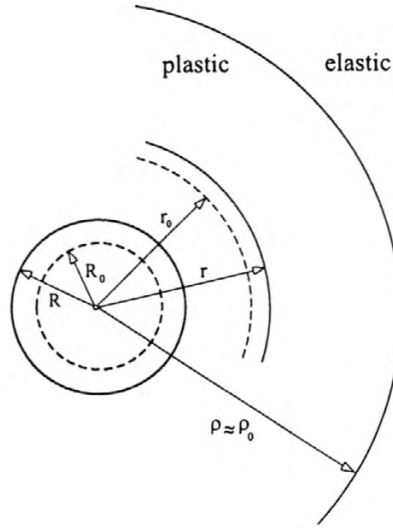
Figure 2: The elastic-plastic interface around the spherical void of initial radius R_0. The radius of the expanded void is R. The initial and current radii of material elements within the plastic zone are r_0 and r. Since deformation is infinitesimal beyond the elastic-plastic interface, its deformed and undeformed radii are nearly equal to each other ($\rho \approx \rho_0$).

The corresponding radial displacement is

$$u = \frac{\sigma}{E}\left[(1-2\nu)r + \frac{1}{2}(1+\nu)\frac{R_0^3}{r^2}\right],$$ (2.5)

where E is Young's modulus and ν is Poisson's ratio of the material.

According to either von Mises or Tresca yield criterion, the plastic deformation commences when

$$\sigma_\theta - \sigma_r = Y.$$ (2.6)

The initial yield stress of the material in uniaxial tension is denoted by Y. Thus, the threshold value of applied stress σ for the onset of

plastic deformation at the surface of the void $(r = R_0)$ is $\sigma_Y = 2Y/3$. With an increase of stress beyond this value, the plastic zone expands outward and at an arbitrary instant of deformation the elastic-plastic boundary has reached the radius ρ (Fig. 2). The corresponding radius of the expanded void is R. A material element within the current plastic zone, which was initially at the radius r_0, is currently at the radius r. We assume that ρ is sufficiently large, so that large strains take place in the vicinity of the void, while infinitesimal strains characterize the elastic zone beyond ρ. This means that $\rho \approx \rho_0$, and similarly for any radius beyond the elastic-plastic boundary. The deformation gradient tensor associated with the spherical expansion of the void, expressed in spherical coordinates, is

$$
\mathbf{F} = \begin{bmatrix} \dfrac{\mathrm{d}r}{\mathrm{d}r_0} & 0 & 0 \\ 0 & \dfrac{r}{r_0} & 0 \\ 0 & 0 & \dfrac{r}{r_0} \end{bmatrix}.
\tag{2.7}
$$

The corresponding volume change of an infinitesimal material element is

$$
\frac{\mathrm{d}V}{\mathrm{d}V_0} = \det \mathbf{F} = \left(\frac{r}{r_0}\right)^2 \frac{\mathrm{d}r}{\mathrm{d}r_0}.
\tag{2.8}
$$

If plastic deformation is assumed to be isochoric, the volume change is entirely due to elastic deformation, and

$$
\frac{\mathrm{d}V - \mathrm{d}V_0}{\mathrm{d}V} = \frac{1 - 2\nu}{E} (\sigma_r + 2\sigma_\theta).
\tag{2.9}
$$

More involved non-linear relationship between the spherical component of stress and volume change could be adopted for high levels of stress (Lubarda, 1986; Lubarda and Richmond, 1999). Combining Eqs. (2.8) and (2.9), there follows

$$
\left(\frac{r_0}{r}\right)^2 \frac{\mathrm{d}r_0}{\mathrm{d}r} = 1 - \frac{1 - 2\nu}{E} (\sigma_r + 2\sigma_\theta).
\tag{2.10}
$$

Incorporating the equilibrium equation (2.1), rewritten as

$$\sigma_r + 2\sigma_\theta = \frac{1}{r^2} \frac{d}{dr} \left(r^3 \sigma_r \right),$$

(2.11)

equation (2.10) becomes

$$r_0^2 \, dr_0 = r^2 dr - \frac{1 - 2\nu}{E} d \left(r^3 \sigma_r \right).$$

(2.12)

Upon integration, using the boundary condition $\sigma_r(R) = 0$, one finds that

$$\sigma_r = \frac{E}{3(1 - 2\nu)} \left(\frac{r^3 - r_0^3}{r^3} - \frac{R^3 - R_0^3}{r^3} \right).$$

(2.13)

This expression holds everywhere in the medium, regardless of the constitutive description in plastic zone $r \leq \rho$.

On the other hand, in the elastic zone $r \geq \rho$ we have

$$\sigma_r = \sigma - \frac{2}{3} Y \frac{\rho^3}{r^3}, \quad \sigma_\theta = \sigma + \frac{1}{3} Y \frac{\rho^3}{r^3},$$

(2.14)

which ensures that $\sigma_\theta(\rho) - \sigma_r(\rho) = Y$, and $\sigma_r + 2\sigma_\theta = 3\sigma$ everywhere in elastic region. Thus, $\sigma_r(\rho) = \sigma - 2Y/3$, and from Eq. (2.13) we obtain

$$\sigma = \frac{2}{3} Y + \frac{E}{3(1 - 2\nu)} \left(\frac{\rho^3 - \rho_0^3}{\rho^3} - \frac{R^3 - R_0^3}{\rho^3} \right).$$

(2.15)

Since the strain is elastic and infinitesimal at the elastic-plastic interface, there is an approximation

$$\frac{\rho^3 - \rho_0^3}{\rho^3} \approx 3\epsilon_\theta(\rho) = \frac{3(1 - 2\nu)}{E} \sigma + \frac{1 + \nu}{E} Y,$$

(2.16)

and the substitution into Eq. (2.15) gives

$$R^3 = R_0^3 + 3(1 - \nu) \frac{Y}{E} \rho^3.$$

(2.17)

At the advanced stages of plastic deformation, when R becomes much greater than R_0, the above result implies that the ratio ρ/R approaches a constant value

$$\frac{\rho}{R} = \left[\frac{E}{3(1-\nu)Y}\right]^{1/3}. \tag{2.18}$$

Equations (2.17) and (2.18) hold for any type of hardening in the plastic zone, but the analysis cannot be pursued further without using the constitutive description of plastic deformation. For an elastoplastic material with a general non-linear hardening the relationship between the applied stress σ and the size of the plastic zone ρ can be determined only numerically. As in the case of a pressurized void, closed form solutions are attainable for two particular material models: an elastic–ideally plastic material, and an incompressible elastic–linearly hardening material. These are derived in the following sections.

3. IDEALLY PLASTIC MATERIAL

In the case of a non-hardening material, we have $\sigma_\theta - \sigma_r = Y$ throughout the plastic zone, and from the equilibrium equation the stress state in the plastic zone ($r \le \rho$) is defined by

$$\sigma_r = Y \ln \frac{r^2}{R^2}, \quad \sigma_\theta = Y\left(1 + \ln \frac{r^2}{R^2}\right). \tag{3.1}$$

Since the stress field in the surrounding elastic region ($r \ge \rho$) is specified by Eq. (2.14), the continuity condition for the radial stress component at the elastic-plastic interface gives

$$\sigma = \frac{2}{3}Y\left(1 + 3\ln\frac{\rho}{R}\right), \quad \rho = R\exp\left(\frac{\sigma}{2Y} - \frac{1}{3}\right). \tag{3.2}$$

The substitution of Eq. (3.2) into Eq. (2.17) furnishes an expression for the current radius of the void in terms of the applied stress

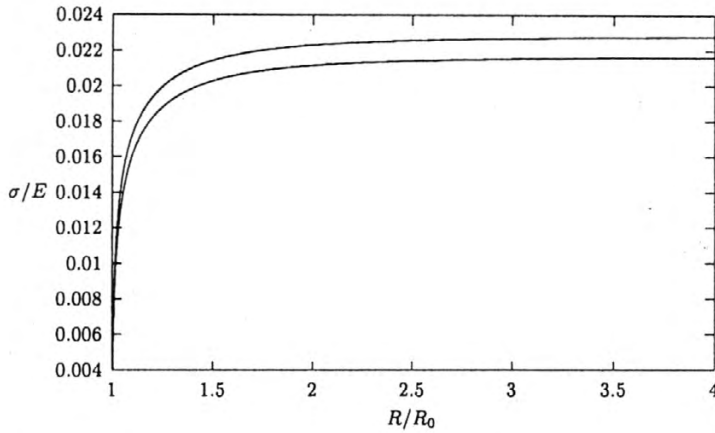$$R = R_0\left[1 - 3(1-\nu)\frac{Y}{E}\exp\left(\frac{3\sigma}{2Y} - 1\right)\right]^{-1/3} \tag{3.3}$$

Figure 3: The normalized stress σ/E vs. expanded void radius R/R_0, according to Eq. (3.3). The results are for $Y/E = 3/500$, and for two values of Poisson's ratio $\nu = 1/3$ (lower curve), and $\nu = 1/2$ (upper curve).

At this stress level, the plastic zone has spread to

$$\rho = R_0 \; \frac{\exp\left(\dfrac{\sigma}{2Y} - \dfrac{1}{3}\right)}{\left[1 - 3(1 - \nu)\dfrac{Y}{E}\exp\left(\dfrac{3\sigma}{2Y} - 1\right)\right]^{1/3}} \; . \tag{3.4}$$

The inverted form, giving σ in terms of ρ, is

$$\sigma = \frac{2Y}{3}\left\{1 - \ln\left[\frac{R_0^3}{\rho^3} + 3(1 - \nu)\frac{Y}{E}\right]\right\} . \tag{3.5}$$

The plot of σ/Y vs. R/R_0 is shown in Fig. 3 for $Y/E = 1/500$, and two values of Poisson's ratio ($\nu = 1/3$ and $\nu = 1/2$). The limiting stress value, obtained as R or ρ increases indefinitely, is

$$\sigma_{\mathrm{cr}} = \frac{2Y}{3}\left\{1 - \ln\left[3(1 - \nu)\frac{Y}{E}\right]\right\} . \tag{3.6}$$

The unlimited void growth under this level of stress is referred to as an unstable cavitation. This stress level is also the critical (bifurcation) stress at which a non-homogeneous deformation bifurcates from the homogeneous one by the sudden void formation. This is further discussed by Chung, Horgan and Abeyaratne (1987), and Huang, Hutchinson and Tvergaard (1991) in the case of an elastoplastic material, and by Ball (1982) and Horgan (1992) in the case of a nonlinear hyperelastic material.

The plots in Fig. 3 reveal a relatively mild effect of elastic compressibility on the value of σ_{cr}. For the considered material properties, an increase of Poisson's ratio from $1/3$ to $1/2$ increases the critical stress by about 5%. The value of the yield stress Y was selected to facilitate the comparison with the results for elastic linearly hardening material model, considered in Section 4. In the latter case, if the plastic hardening modulus is k and the initial yield stress is Y_0, the average yield stress in the range of plastic strain up to 0.5 is $Y = Y_0 + k/4$. Consequently, for $Y_0 = E/500$ and $k = E/50$ we took $Y = 3Y_0$, which was used in calculations for the plots shown in Fig. 3. The critical stress is in this case about 2.3% of Young's modulus E, or 7% of the shear modulus (in the case of an incompressible material). It should also be pointed out that σ_{cr} is an increasing function of Y, as expected on the physical ground. For example, if Y is increased from $E/500$ to twice that value, the stress required for the cavitation instability or void nucleation increases by about 80%.

4. INCOMPRESSIBLE LINEARLY HARDENING MATERIAL

If material is both elastically and plastically incompressible, we have $\det \mathbf{F} = 1$ in Eq. (2.8), and

$$r^3 - r_0^3 = R^3 - R_0^3 = \rho^3 - \rho_0^3 = \frac{3Y}{2E}\rho^3 \qquad (4.1)$$

The deformation gradient tensor is in this case

$$\mathbf{F} = \begin{bmatrix} \dfrac{r_0^2}{r^2} & 0 & 0 \\ 0 & \dfrac{r}{r_0} & 0 \\ 0 & 0 & \dfrac{r}{r_0} \end{bmatrix}. \tag{4.2}$$

By using the multiplicative decomposition of the deformation gradient into its elastic and plastic parts $(\mathbf{F} = \mathbf{F}_e \cdot \mathbf{F}_p)$, we can write

$$\mathbf{F} = \begin{bmatrix} \dfrac{r_p^2}{r^2} & 0 & 0 \\ 0 & \dfrac{r}{r_p} & 0 \\ 0 & 0 & \dfrac{r}{r_p} \end{bmatrix} \cdot \begin{bmatrix} \dfrac{r_0^2}{r_p^2} & 0 & 0 \\ 0 & \dfrac{r_p}{r_0} & 0 \\ 0 & 0 & \dfrac{r_p}{r_0} \end{bmatrix} \tag{4.3}$$

The logarithmic strain

$$\mathbf{E} = \begin{bmatrix} -2\ln\dfrac{r}{r_0} & 0 & 0 \\ 0 & \ln\dfrac{r}{r_0} & 0 \\ 0 & 0 & \ln\dfrac{r}{r_0} \end{bmatrix} \tag{4.4}$$

can then be additively decomposed into its elastic and plastic parts as $\mathbf{E} = \mathbf{E}_e + \mathbf{E}_p$, i.e.,

$$\mathbf{E} = \begin{bmatrix} -2\ln\dfrac{r}{r_p} & 0 & 0 \\ 0 & \ln\dfrac{r}{r_p} & 0 \\ 0 & 0 & \ln\dfrac{r}{r_p} \end{bmatrix} + \begin{bmatrix} -2\ln\dfrac{r_p}{r_0} & 0 & 0 \\ 0 & \ln\dfrac{r_p}{r_0} & 0 \\ 0 & 0 & \ln\dfrac{r_p}{r_0} \end{bmatrix} \tag{4.5}$$

For the proportional loading, the generalized plastic strain (Lubarda, 2002) is

$$\bar{E}_{\mathrm{p}} = \left(\frac{2}{3}\, \mathbf{E}_{\mathrm{p}} : \mathbf{E}_{\mathrm{p}}\right)^{1/2} = 2\ln\frac{r_{\mathrm{p}}}{r_0}\,. \tag{4.6}$$

The trace product is denoted by : sign. If the material is linearly hardening with respect to this strain measure, the equivalent yield stress at an arbitrary stage of deformation can be expressed as

$$\sigma_\theta - \sigma_r = Y + 2k\,\ln\frac{r_{\mathrm{p}}}{r_0} = Y + 2k\left(\ln\frac{r}{r_0} - \ln\frac{r}{r_{\mathrm{p}}}\right), \tag{4.7}$$

where k is the hardening modulus. By using Hooke's type law for the elastic component of strain

$$\mathbf{E}_{\mathrm{e}} = \frac{3}{2E}\left[\boldsymbol{\sigma} - \frac{1}{3}\,(\mathrm{tr}\,\boldsymbol{\sigma})\,\mathbf{I}\right], \tag{4.8}$$

it follows that

$$\ln\frac{r}{r_{\mathrm{p}}} = \frac{1}{2E}\,(\sigma_\theta - \sigma_r)\,. \tag{4.9}$$

The substitution of Eq. (4.9) into Eq. (4.7) yields

$$\sigma_\theta - \sigma_r = \hat{Y} + 2\hat{k}\,\ln\frac{r}{r_0}\,, \tag{4.10}$$

with the abbreviations

$$\hat{Y} = \frac{Y}{1 + k/E}\,, \qquad \hat{k} = \frac{k}{1 + k/E}\,. \tag{4.11}$$

The distinction between the barred and non-barred quantities is important for strong hardening rates and higher values of the ratio k/E. Physically, the stress $\hat{Y}$ and the hardening modulus $\hat{k}$ appear in the relationship between uniaxial stress and total strain ($\sigma = \hat{Y} + \hat{k}E$), while Y and k appear in the relationship between uniaxial stress and plastic strain ($\sigma = Y + kE_{\mathrm{p}}$).
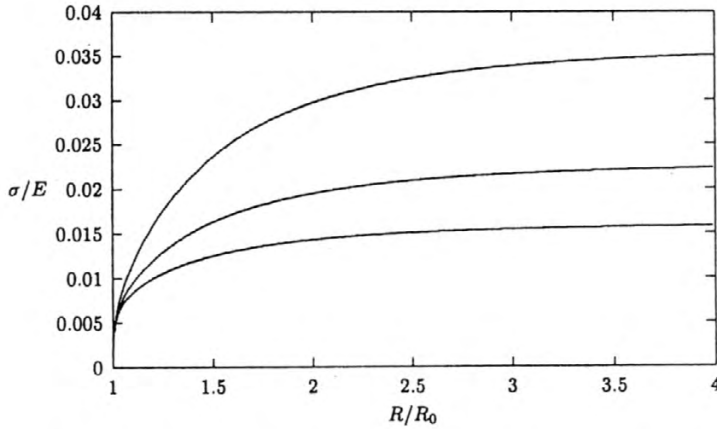
Figure 4: The normalized stress σ/E *vs.* the expanded void radius R/R_0, according to Eq. (4.14). The results are for $Y/E = 1/500$, and for three values of the hardening modulus $k/E = 1/100, 1/50$, and $1/25$ (from lower to upper curve).

When Eq. (4.10) is introduced into Eq. (2.1), the integration gives

$$\sigma_r = 2\hat{Y} \ln \frac{r}{R} + \frac{4\hat{k}}{3} \int_R^r \ln \frac{r^3}{r_0^3} \frac{\mathrm{d}r}{r} \,, \tag{4.12}$$

or, in view of Eq. (4.1),

$$\sigma_r = 2\hat{Y} \ln \frac{r}{R} + \frac{4\hat{k}}{9} \sum_{n=1}^{\infty} \frac{1}{n^2} \left[\left(\frac{R^3 - R_0^3}{R^3} \right)^n - \left(\frac{R^3 - R_0^3}{r^3} \right)^n \right]. \tag{4.13}$$

Evaluating at $r = \rho$, and equating the result with $\sigma_r(\rho) = \sigma - 2Y/3$, following from Eq. (2.14), provides an expression for the applied stress σ in terms of the plastic zone radius ρ. This is

$$\sigma = \frac{2}{3}Y + 2\hat{Y} \ln \frac{\rho}{R} + \frac{4\hat{k}}{9} \sum_{n=1}^{\infty} \frac{1}{n^2} \left[\left(\frac{R^3 - R_0^3}{R^3} \right)^n - \left(\frac{3Y}{2E} \right)^n \right]. \quad (4.14)$$

The radius R of the expanded void is given in terms of ρ by Eq. (4.1). The plot of σ/Y vs. R/R_0 is shown in Fig. 4 (for $Y/E = 1/500$ and for three indicated values of the ratio k/E). If the plastic zone surrounding the void has spread to a large radius ρ, we have $R^3 >> R_0^3$, and neglecting higher than linear terms in $3Y/2E$, there follows

$$\sigma_{\mathrm{cr}} = \frac{2Y/3}{1 + k/E} \left(1 + \ln \frac{2E}{3Y} + \frac{\pi^2}{9} \frac{k}{Y} \right). \quad (4.15)$$

This is the critical stress for cavitation instability in an incompressible elastic -linearly hardening material. If the ratio $k/E << 1$, the above result coincides with the result of Bishop, Hill and Mott (1945) for a pressurized spherical cavity in an infinite solid. This is so because the solutions for a pressurized spherical void and a spherical void under remote triaxial tension differ by a state of uniform spherical stress throughout the medium, which for an incompressible material has no effect on the deformation field. If $k = 0$ is substituted in Eq. (4.15), and $\nu = 1/2$ in Eq. (3.6), the two expressions give the critical stress for cavitation instability in an incompressible elastic-ideally plastic material. Figure 4 reveals that for $k = E/50$ the critical stress is about 2.3% of Young's modulus E, which is in agreement with ideally plastic calculations from Section 3, with an effective yield stress of $3Y$. For the hardening modulus $k = E/25$, the critical stress increases to about 3.5% of E, while it is about 1.6% of E for $k = E/100$. In this context it should be pointed out that experimentally observed values of the spalling strength for ordinary polycrystalline materials are in the range of several GPa's. For example, the spalling strength of a pure polycrystalline copper is about 2.5 GPa, and of monocrystalline copper about 5 GPa (due to absence of grain boundaries, which promote cavitation).

5. CYLINDRICAL VOID GROWTH

Consider now a cylindrical void of initial radius R_0 in an isotropic infinite medium under remote biaxial tension σ. Assume the plane strain conditions. The stress state at an arbitrary point consists of the radial stress σ_r, the hoop stress σ_θ, and the longitudinal stress σ_z. Due to cylindrical symmetry, the stress components depend only on the radial distance r. In the absence of body forces the equilibrium equation is

$$\frac{d\sigma_r}{dr} - \frac{1}{r}(\sigma_\theta - \sigma_r) = 0. \tag{5.1}$$

If the material response is within the infinitesimal elastic range, the compatibility equation reduces to

$$\frac{d}{dr}(\sigma_r + \sigma_\theta) = 0, \quad \text{i.e.,} \quad \sigma_r + \sigma_\theta = 2\sigma. \tag{5.2}$$

Combining Eqs. (5.1) and (5.2), it follows that

$$\sigma_r = \sigma\left(1 - \frac{R_0^2}{r^2}\right), \quad \sigma_\theta = \sigma\left(1 + \frac{R_0^2}{r^2}\right). \tag{5.3}$$

The longitudinal stress is $\sigma_z = 2\nu\sigma$, and the radial displacement

$$u = \frac{\sigma}{2G}\left[(1 - 2\nu)r + \frac{R_0^2}{r}\right]. \tag{5.4}$$

According to the von Mises yield criterion, the plastic deformation commences when

$$\frac{3}{4}(\sigma_\theta - \sigma_r)^2 + \left(\sigma_z - \frac{\sigma_r + \sigma_\theta}{2}\right)^2 = Y^2. \tag{5.5}$$

Thus, the threshold value of applied stress σ for the onset of plastic deformation at the surface of the void is

$$\sigma_Y = \frac{Y}{[3 + (1 - 2\nu)^2]^{1/2}}. \tag{5.6}$$

With an increase of stress beyond this value, the plastic zone expands outward and at an arbitrary instant of deformation the elastic-plastic boundary has reached the radius ρ. The deformation gradient tensor, associated with a cylindrical expansion of the void and expressed in cylindrical coordinates, becomes

$$
\mathbf{F} = \begin{bmatrix}
\dfrac{\mathrm{d}r}{\mathrm{d}r_0} & 0 & 0 \\[2mm]
0 & \dfrac{r}{r_0} & 0 \\[2mm]
0 & 0 & 1
\end{bmatrix}. \tag{5.7}
$$

The corresponding volume change of an infinitesimal material element is

$$
\frac{\mathrm{d}V}{\mathrm{d}V_0} = \det \mathbf{F} = \frac{r}{r_0}\frac{\mathrm{d}r}{\mathrm{d}r_0}. \tag{5.8}
$$

If plastic deformation is assumed to be isochoric, the volume change is entirely due to elastic deformation, so that

$$
\frac{\mathrm{d}V - \mathrm{d}V_0}{\mathrm{d}V} = \frac{1}{E}\left[(1-\nu)(\sigma_r + \sigma_\theta) - 2\nu\sigma_z\right]. \tag{5.9}
$$

The closed form analysis can be pursued further for an elastically incompressible material ($\nu = 1/2$). The longitudinal stress σ_z is then an arithmetic mean of the other two stress components throughout the medium, and

$$
r^2 - r_0^2 = R^2 - R_0^2 = \rho^2 - \rho_0^2. \tag{5.10}
$$

In the elastic zone $r \geq \rho$, the stress components are

$$
\sigma_r = \sigma - \frac{Y}{\sqrt{3}}\frac{\rho^2}{r^2}, \quad \sigma_\theta = \sigma + \frac{Y}{\sqrt{3}}\frac{\rho^2}{r^2}, \quad \sigma_z = \sigma. \tag{5.11}
$$

They satisfy the yield condition (5.5) at the elastic-plastic interface $r = \rho$, and the condition $\sigma_r + \sigma_\theta = 2\sigma$ everywhere in the elastic region. Since

the strain is elastic and infinitesimal at the elastic-plastic interface, we can write

$$\frac{\rho^2 - \rho_0^2}{\rho^2} \approx 2\epsilon_\theta(\rho) = \frac{\sqrt{3}Y}{E}, \tag{5.12}$$

and the substitution into Eq. (5.10) gives

$$R^2 = R_0^2 + \frac{\sqrt{3}Y}{E}\rho^2. \tag{5.13}$$

At the advanced stages of plastic deformation, when R becomes much greater than R_0, the ratio ρ/R approaches a constant value

$$\frac{\rho}{R} = \left(\frac{E}{\sqrt{3}Y}\right)^{1/2}. \tag{5.14}$$

Equations (5.13) and (5.14) hold regardless of the type of material hardening in the plastic zone.

The deformation gradient tensor for the void expansion in an incompressible material is

$$\mathbf{F} = \begin{bmatrix} \dfrac{r_0}{r} & 0 & 0 \\ 0 & \dfrac{r}{r_0} & 0 \\ 0 & 0 & 1 \end{bmatrix} \tag{5.15}$$

By using the multiplicative decomposition of the deformation gradient into its elastic and plastic parts $(\mathbf{F} = \mathbf{F}_e \cdot \mathbf{F}_p)$, we have

$$\mathbf{F} = \begin{bmatrix} \dfrac{r_p}{r} & 0 & 0 \\ 0 & \dfrac{r}{r_p} & 0 \\ 0 & 0 & 1 \end{bmatrix} \cdot \begin{bmatrix} \dfrac{r_0}{r_p} & 0 & 0 \\ 0 & \dfrac{r_p}{r_0} & 0 \\ 0 & 0 & 1 \end{bmatrix} \tag{5.16}$$

The corresponding logarithmic strain

$$\mathbf{E} = \begin{bmatrix} -\ln\dfrac{r}{r_0} & 0 & 0 \\ 0 & \ln\dfrac{r}{r_0} & 0 \\ 0 & 0 & 0 \end{bmatrix} \tag{5.17}$$

can then be additively decomposed as $\mathbf{E} = \mathbf{E}_e + \mathbf{E}_p$, i.e.,

$$\mathbf{E} = \begin{bmatrix} -\ln\dfrac{r}{r_p} & 0 & 0 \\ 0 & \ln\dfrac{r}{r_p} & 0 \\ 0 & 0 & 0 \end{bmatrix} + \begin{bmatrix} -\ln\dfrac{r_p}{r_0} & 0 & 0 \\ 0 & \ln\dfrac{r_p}{r_0} & 0 \\ 0 & 0 & 0 \end{bmatrix}. \tag{5.18}$$

If the material is linearly hardening with respect to the generalized plastic strain

$$\bar{\mathbf{E}}_p = \left(\frac{2}{3}\mathbf{E}_p : \mathbf{E}_p\right)^{1/2} = \frac{2}{\sqrt{3}}\ln\frac{r_p}{r_0}, \tag{5.19}$$

the equivalent yield stress $\sqrt{3}(\sigma_\theta - \sigma_r)/2$ at an arbitrary stage of deformation is

$$\frac{\sqrt{3}}{2}(\sigma_\theta - \sigma_r) = Y + \frac{2k}{\sqrt{3}}\ln\frac{r_p}{r_0} = Y + \frac{2k}{\sqrt{3}}\left(\ln\frac{r}{r_0} - \ln\frac{r}{r_p}\right). \tag{5.20}$$

By using Hooke's type law for the elastic component of strain,

$$\ln\frac{r}{r_p} = \frac{3}{4E}(\sigma_\theta - \sigma_r), \tag{5.21}$$

the substitution into Eq. (5.20) yields

$$\sigma_\theta - \sigma_r = \hat{Y} + \hat{k}\ln\frac{r}{r_0}. \tag{5.22}$$

The abbreviations are here used

$$\hat{Y} = \frac{2Y/\sqrt{3}}{1 + k/E}, \quad \hat{k} = \frac{4k/3}{1 + k/E}. \tag{5.23}$$

When Eq. (5.22) is introduced into Eq. (5.1), the integration gives

$$\sigma_r = \hat{Y} \ln \frac{r}{R} + \frac{\hat{k}}{4} \sum_{n=1}^{\infty} \frac{1}{n^2} \left[\left(\frac{R^2 - R_0^2}{R^2} \right)^n - \left(\frac{R^2 - R_0^2}{r^2} \right)^n \right]. \tag{5.24}$$

Evaluating this at $r = \rho$, and equating the result with $\sigma_r(\rho) = \sigma - Y/\sqrt{3}$, following from Eq. (5.11), provides an expression for the applied stress σ in terms of the plastic zone radius ρ. This is

$$\sigma = \frac{Y}{\sqrt{3}} + \hat{Y} \ln \frac{\rho}{R} + \frac{\hat{k}}{4} \sum_{n=1}^{\infty} \frac{1}{n^2} \left[\left(\frac{R^2 - R_0^2}{R^2} \right)^n - \left(\frac{\sqrt{3}Y}{E} \right)^n \right]. \tag{5.25}$$

The radius of the expanded void R is given in terms of ρ by Eq. (5.13). If the plastic zone around the void has spread to a large extent, we have

$$\sigma_{\mathrm{cr}} = \frac{Y/\sqrt{3}}{1 + k/E} \left(1 + \ln \frac{E}{\sqrt{3}Y} + \frac{\pi^2}{18} \frac{\sqrt{3}k}{Y} \right). \tag{5.26}$$

This is the critical stress for a cylindrical cavitation instability in an incompressible elastic–linearly hardening material. If $k \ll E$, the result reduces to that of Hill (1950) for a pressurized cylindrical void in an infinitely extended material.

6. DISCUSSION

To first order accuracy, the inclusion of the term k/E decreases the calculated value of the critical stress for k/E percent relative to the value obtained when this term is omitted. Thus, the effect of the ratio of the hardening to elastic modulus on the critical or bifurcation stress, for both spherical and cylindrical void cavitation, is important only for exceedingly strong hardening rates, reaching the values as high

as $0.1E$. Normally, such high values of k are not characteristic of ordinary structural metals, but may occur in materials designed to initially yield and then strongly resist further plastic deformation. The nanocrystalline materials produced by severe plastic deformation, such as equal-channel angular pressing, high pressure torsion, or repetitive corrugation and straightening, are characterized by grain size of the order of 100 nanometers and extraordinary combination of strength and ductility properties. For example, nanocrystalline pure Ti processed by severe plastic deformation has hardening rates in the range of 2 − 10 GPa, depending on the grain size, while preserving its ductility in the range of 10 − 30% (Valiev *et al.*, 2000). Such high strength and ductility properties are the consequence of different dislocation structures and different mechanisms of plastic deformation that take place in nanocrystalline *vs.* coarse grain size crystalline materials. This certainly affects the void nucleation and growth under tensile loading, and the material spalling strength under dynamic, explosive or impact loading (Meyers *et al.*, 2003). The results presented in this paper are intended for such applications. The worthwhile continuation of this research is to express the yield stress and the hardening rates in terms of the nanocrystalline grain size, and adjust the introduced material parameters according to available experimental data. This is related to a long-standing problem of the theoretical verification and derivation of the Hall-Petch type relationship between the flow stress and grain size in different metals and alloy systems (e.g., Meyers and Chawla, 1999). A discrete dislocation model for the calculation of the critical stress required for void nucleation has recently been proposed and analyzed by Lubarda, Schneider, Meyers, *et al.* (2003).

REFERENCES

Ball, J.M. (1982) Discontinous equilibrium solutions and cavitation in nonlinear elasticity. *Phil. Trans. R. Soc. Lond.* **A306**, 557–610.

Belak, J. (1998) In *Shock Compression of Condensed Matter – 1997. AIP Conference Proceedings* **429** (Eds. S. C. Schmidt, D. P. Dandekar and J.W. Forbes), p. 211. American Inst. of Phys. Press, Woodbury, N.Y.

Benson, D.J. (1993) An analysis of void distribution effects on the dynamic growth and coalescence of voids in ductile metals. *J. Mech. Phys. Solids* **41**, 1285–1308.

Bishop, R.F., Hill, R. and Mott, N.F. (1945) The theory of indentation and hardness tests. *Proc. Phys. Soc.* **57**, 147–159.

Budiansky, B., Hutchinson, J.W. and Slutsky, S. (1982) Void growth and collapse in viscous solids. In *Mechanics of Solids: The Rodney Hill 60th Anniversary Volume* (Eds. H. G. Hopkins and M. J. Sewell), pp. 13–45. Pergamon Press, Oxford.

Carroll, M.M. and Holt, A.C. (1972) Static and dynamic pore-collapse relations for ductile porous materials. *J. Appl. Phys.* **43**, 1626–1636.

Chakrabarty, J. (1987) *Theory of Plasticity*. McGraw-Hill, New York.

Chung, D.-T., Horgan, C.O. and Abeyaratne, R. (1987) A note on a bifurcation problem in finite plasticity related to void nucleation. *Int. J. Solids Struct.* **23**, 983–988.

Cortés, R. (1992) Dynamic growth of microvoids under combined hydrostatic and deviatoric stresses. *Int. J. Solids Struct.* **29**, 1637–1645.

Cuitiño, A.M. and Ortiz, M. (1996) Ductile fracture by vacancy condensation in F.C.C. crystals. *Acta mater.* **44**, 427–436.

Gurson, A.L. (1977) Continuumtheory of ductile rapture by void nucleation and growth – Part I: Yield criteria and flow rules for porous

ductile media. *J. Engng. Mater. Tech.* **99**, 2–15.

Hill, R. (1950) *The Mathematical Theory of Plasticity.* Oxford Univ. Press, London.

Hopkins, H.G. (1960) Dynamic expansion of spherical cavities in metals. In *Progress in Solid Mechanics* **1** (Eds. I.N. Sneddon and R. Hill), pp. 81–164. North-Holland, Groningen.

Horgan, C.O. (1992) Void nucleation and growth for compressible non-linearly elastic materials: an example. *Int. J. Solids Struct.* **29**, 279–291.

Horgan, C.O. and Polignone, D.A. (1996) Cavitation in non-linearly elastic solids: a review. *Appl. Mech. Rev.* **48**, 471–485.

Huang, Y., Hutchinson, J.W. and Tvergaard, V. (1991) Cavitation instabilities in elastic-plastic solids. *J. Mech. Phys. Solids* **39**, 223–241.

Johnson, J.N. (1981) Dynamic fracture and spallation in ductile solids. *J. Appl. Phys.* **52**, 2812–2825.

Kassner, M.E. and Hayes, T.A. (2003) Creep cavitation in metals. *Int. J. Plasticity* **19**, in press.

Koplik, J. and Needleman, A. (1988) Void growth and coalescence in porous plastic solids. *Int. J. Solids Struct.* **24**, 835–853.

Lubarda, V.A. (1986) Finite compression of solids - second order thermoelastic analysis. *Int. J. Solids Struct.* **22**, 1517–1524.

Lubarda, V.A. (2002) *Elastoplasticity Theory*, CRC Press, Boca Raton, FL.

Lubarda, V.A., Schneider, M.S., Meyers, M.A., *et al.* (2003) Void Initiation and Growth in Spalling, *Dynamic Deformation: Constitutive Modeling, Grain Size, and Other Effects*, 2003 TMS Annual Meeting, San Diego.

Lubarda, V.A. and Ricmond, O. (1999) Second-order elastic analysis of dilute distribution of spherical inclusions. *Mech. Mater.* **31**, 1–8.

Lubliner, J. (1990) *Plasticity Theory*, Macmillan, New York.

McClintock, F.A. (1968) A criterion for ductile fracture by growth of holes. *J. Appl. Mech.* **35**, 363–371.

Meyers, M.A. and Aimone, C.T. (1983) Dynamic fracture (spalling) of metals. *Progress in Materials Science* **28**, 1–96.

Meyers, M.A. and Chawla, K.M. (1999) *Mechanical Behavior of Materials*, Prentice-Hall, New York.

Meyers, M.A., *et al.* (2003) Laser-induced shock compression of monocrystalline copper: characterization and analysis. *Acta mater.*, in press.

Meyers, M.A., Murr, L.E. and Staudhammer, K.P. (1986) *Shock Wave and High Strain-Rate Phenomena in Materials*. Dekker, New York.

Needleman, A. (1972) Void growth in an elastic-plastic medium. *J. Appl. Mech.* **39**, 964–970.

Needleman, A., Tvergaard, V. and Hutchinson, J. W. (1992) Void growth in plastic solids. In *Topics in Fracture and Fatigue* (Ed. A.S. Argon), pp. 145-178. Springer-Verlag, New York.

Ortiz, M. and Molinari, A. (1992) Effect of strain hardening and rate sensitivity on the dynamic growth of a void in a plastic material. *J. Appl. Mech.* **59**, 48–53.

Pardoen, T. and Hutchinson, J.W. (2000) An extended model for void growth and coalescence. *J. Mech. Phys. Solids* **48**, 2467–2512.

Polignone, D.A. and Horgan, C.O. (1993) Effects of material anisotropy and inhomogeneity on cavitation for composite incompressible anisotropic nonlinearly elastic spheres. *Int. J. Solids Struct.* **30**, 3381–3416.

Rice, J.R. and Tracey, D.M. (1969) On the ductile enlargement of voids in triaxial stress fields. *J. Mech. Phys. Solids* **17**, 201–217.

Rudd, R.E. and Belak, J.F. (2002) Void nucleation and associated plasticity in dynamic fracture of polycrystalline copper: an atomis-

tic simulation. *Comp. Mater. Sci.* **24**, 148–153.

Stuart, C.A. (1985) Radially symmetric cavitation for hyperelastic materials. *Ann. Inst. Henri Poincaré-Analyse non Linéaire* **2**, 33-66.

Tvergaard, V. (1990) Material failure by void growth to coalescence. *Adv. Appl. Mech.* **27**, 83–151.

Valiev, R.Z., Islamgaliev, R.K. and Alexandrov, I.V. (2000) Bulk nanostructured materials from severe plastic deformation. *Prog-ress in Materials Science* **45**, 103–189.

Wang, Z.P. (1994) Void growth and compaction relations for ductile porous materials under intense dynamic general loading conditions. *Int. J. Solids Struct.* **31**, 2139–2150.

Williams, M.L. and Schapery, R.A. (1965) Spherical flaw instability in hydrostatic tension. *Int. J. Fract. Mech.* **1**, 64–71.

Wu, X.Y., Ramesh, K.T. and Wright, T.W. (2003) The dynamic growth of a single void in a viscoplastic material under transient hydrostatic loading. *J. Mech. Phys. Solids* **51**, 1–26.